Supplementary information

Tailoring hydron-halogen bond networks in heptazine architectures for controlled fabrication of high-performance C-doped porous carbon nitride photocatalyst

Jiawei Xia,[a] Yuming He,[a] Yongke Hu,[b] Ting Hu,[c] Yuxuan Tong,[a] Xingyue Qian,[a] Xue Chen,[a] Guangyu He[a]* and Haiqun Chen[a]*

[a] Key Laboratory of Advanced Catalytic Materials and Technology, Advanced Catalysis and Green Manufacturing Collaborative Innovation Center, Changzhou University, Changzhou, Jiangsu Province 213164, China

[b] National & Local Joint Engineering Research Center for Mineral Salt Deep Utilization, Huaiyin Institute of Technology, Huaian, Jiangsu Province 223003, China

[c] Department of Applied Physics and MIIT Key Laboratory of Semiconductor Microstructure and Quantum Sensing, Nanjing University of Science and Technology, Nanjing, Jiangsu Province 210094, China

Email for corresponding authors:

Guangyu He: hegy@cczu.edu.cn

Haiqun Chen: chenhq@cczu.edu.cn

Experimental section

Materials and reagents

Melamine (M, ≥99%), 2,4,6-triaminopyrimidine (TAP, ≥98.0%), Chloroplatinic acid solution (H_2PtCl_6, 8wt% in H_2O), triethanolamine (TEOA, A.R.) were purchased from Shanghai Aladdin Reagent Co., Ltd. Hydrochloric acid (HCl, 36~38%) was supplied by Sinopharm Chemical Reagent Co., Ltd. All chemicals and reagents were used as received without post-treatment unless stated otherwise. And the water used throughout the whole experiment is deionized (DI) water, which is obtained from a Millipore Direct-Q 3 system (18.2 MΩ cm resistivity at room temperature).

Catalyst preparation

10 g of melamine was first mixed thoroughly with a certain amount of 2,4,6-triaminopyrimidine via continuous grinding in an agate mortar. The mixture was then placed in the tube furnace for a 6-h prepolymerization at 425°C under N_2 atmosphere, yielding C-doped melem, labelled as $MTAP_x$ (x represents to the feeding of TAP *vs.* 10 g of M). To prepare the H−Cl bonded supramolecular precursor, 0.5 g of $MTAP_x$ was dispersed in HCl solution, where the concentration was adjusted by mixing y mL of concentrated HCl solution with (25−y) mL of DI water. After continuous stirring overnight followed by a natural evaporation in a petri dish, white supramolecule was obtained, marked as $MTAP_xCl_y$. The reference supramolecular assembly prepared without the addition of TAP was labelled as $MelCl_y$. The carbon nitride samples were obtained by annealing the precursors at 550°C for 4 h in air with the ramping rate of 5°C min^{-1}. To mark the CN samples, "CN-" was added in front of each precursor, such as CN-$MelCl_1$, CN-$MTAP_xCl_y$. In addition, CN-M and CN-melem were synthesized for comparison by simply calcinating melamine or melem under the above same condition.

Characterization

The morphologies of the catalysts were characterized by transmission electron microscopy (TEM, JEM-2100F, operated at U_0 = 120 kV) and scanning electron microscopy (SEM, JSM-7800F, operated at U_0 = 3.0 kV). The crystalline structures of

the catalysts were determined via X-ray powder diffraction (XRD) patterns recorded on a X'Pert PRO MPD powder diffractometer (Cu Kα, λ = 0.154178nm) with 2θ ranging from 10° to 60°. The apparent specific surface area of CN materials was determined based on the Brunauer-Emmett-Teller (BET) model applied to the adsorption branch of the N_2 adsorption-desorption isotherms, recorded on an AUTOSORB IQ Autosorb BET analyzer at 77 K. The chemical environment of the elements in the CN materials was characterized via X-ray photoelectron spectroscopy (XPS, Thermo Scientific K-Alpha, Al Kα, 1486.6 eV). As for the optical properties, Fourier-transform infrared spectroscopy (FTIR) was recorded on Thermo Scientific Nicolet iS5 (KBr window, diamond iD7 ATR optical base) for the analysis of the functional groups and bond information of the catalyst. UV-vis diffuse reflection spectrum (DRS) was recorded on a Shimadzu UV-2700 spectrophotometer to characterize the light absorption properties, where the optical bandgap of CN materials can be estimated based on the Tauc plot from the spectra. Photoluminescence (PL) spectra were recorded on a fluorescence spectrometer (F-700) excited at a wavelength of 360 nm.

Test for photocatalytic H_2 evolution reaction

Photocatalytic H_2 evolution reaction was carried out in a custom-built sealed quartz jacketed beaker equipped with a water-cooling system maintained at 25°C. A 300 W Xe lamp with a 420 nm cut filter was employed as the light source (~1110 mW cm^{-2}). Typically, 30 mg of the CN catalyst was dispersed in 34.2 mL of DI water under continuous sonication until uniform, followed by adding 3.8 mL of TEOA (serving as the whole scavenger) and 40 μL of H_2PtCl_6 solution into the suspension. The mixture was then transferred to the sealed reactor and purged with Ar to remove the residual air. The mixture was stirred continuously for the whole measurement. Upon light irradiation, the Pt nanoparticles were photo deposited onto the surface of CN as the cocatalyst within the first 0.5 h. The amount of produced H_2 was monitored every 1 h via gas chromatography (GC, SP-6890). The apparent quantum efficiency (AQE) was measured by conducting the reaction under nonochromatic light (λ = 405, 435 and 450

nm) using the equation below:

$$AQE = \frac{2 \times number\ of\ evolved\ H_2\ molecules}{number\ of\ incident\ photons} \times 100\%$$

(Photo)electrochemical test

(Photo)electrochemical tests were performed on a CHI920C electrochemical potentiostat equipped with a three-electrode system, using Pt wire, Hg/HgO and CN coated FTO glass as the counter, reference, and working electrodes, respectively. 1.0 M Na_2SO_4 aqueous solution (pH ≈ 6.92) was served as the electrolyte. To prepare the working electrode, 10 mg of CN powder was dispersed in the mixed solution composed of 100 μL of DI water and 100 μL of isopropanol assessed under continuous sonication until homogeneous. After that, 50 μL of the catalyst ink was drop casted on to the surface of the FTO glass, and dried on a heating plate at 60°C. To enhance the adhesion of the CN layer on the FTO coated glass, the working electrode was further calcinated at 250°C for 1 h. In addition, the area of the CN layer coated on FTO glass was fixed as 1 cm^2 so as to reach a minimum influence of the objective factors. The potential was converted to *vs.* NHE (normal hydrogen electrode) according to the Nernst equation: $E_{RHE} = E_{Hg/HgO} + 0.0591 \times pH + 0.098$.

DFT calculation

The calculations were performed using the spin polarized density functional theory (DFT) in the generalized gradient approximation (GGA), implemented by the VASP code, in which the projected augmented wave method and the Perdew-Burke-Ernzerhof (PBE) exchange-correlation functional were employed. The isolated molecules are simulated by adding vacuum space which is set to be more than 15 Å. The geometry structure optimization was performed using the conjugated gradient minimization scheme. The convergence criteria for electronic and ionic relaxations are 10^{-5} eV/atom and 0.005 eV/Å, respectively. The energy cut-off for the plane wavefunction is 520 eV. The long range van der Waals interactions are described by a semi-empirical DFT-D3 method.

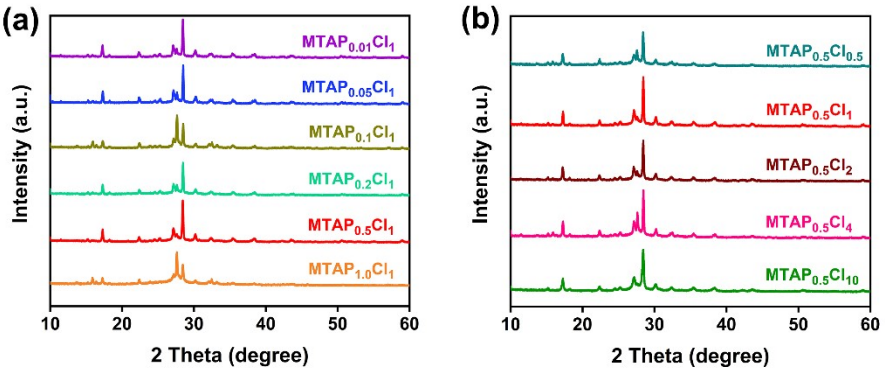

Figure S1. XRD patterns of (a) $MTAP_xCl_1$ and (b) $MTAP_{0.5}Cl_y$ supramolecular precursors synthesized with varied TAP and HCl feedings, respectively.

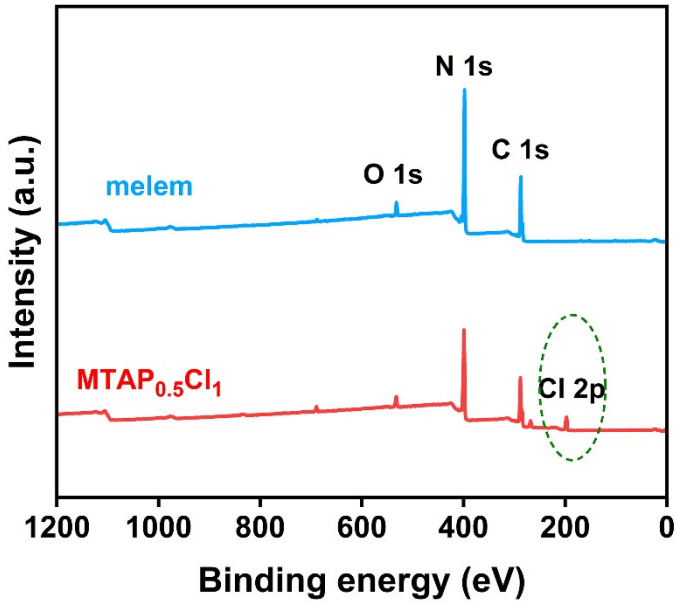

Figure S2. Survey XPS spectra of melem and $MTAP_{0.5}Cl_1$.

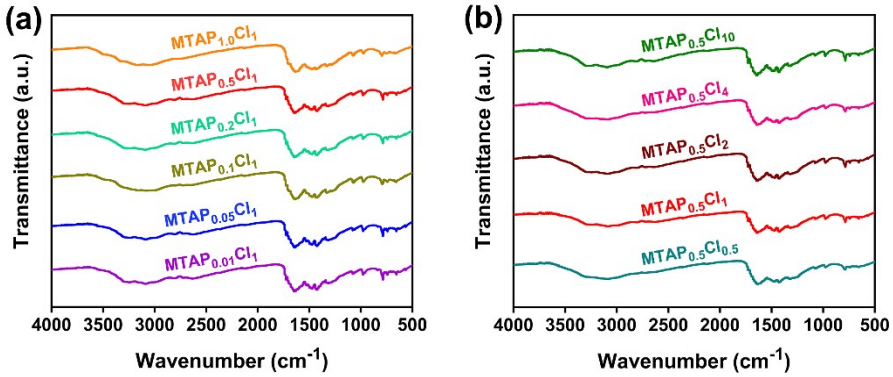

Figure S3. FTIR spectra of (a) $MTAP_xCl_1$ and (b) $MTAP_{0.5}Cl_y$ supramolecular precursors synthesized with varied TAP and HCl feedings, respectively.

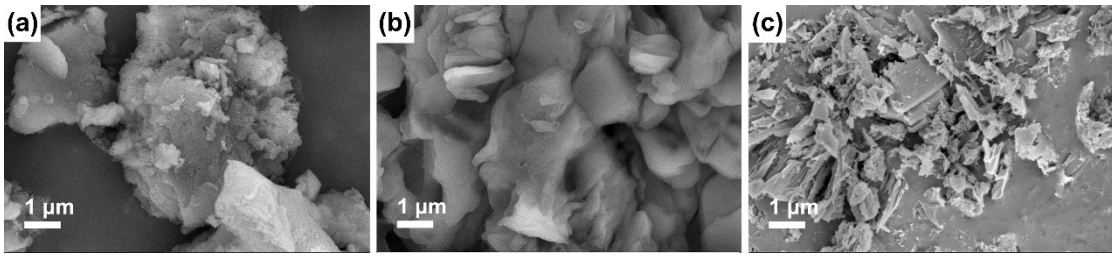

Figure S4. Morphological characterization: SEM images of (a) CN-M, (b) CN-melem and (c) CN-$MelCl_1$.

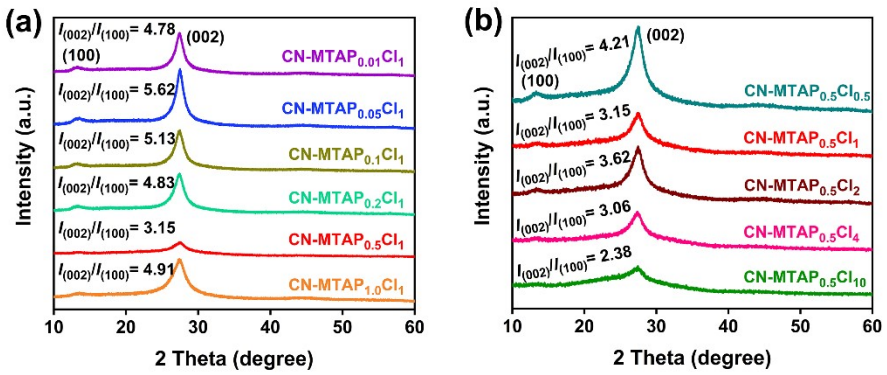

Figure S5. XRD patterns of CN samples synthesized from (a) $MTAP_xCl_1$ and (b) $MTAP_{0.5}Cl_y$ supramolecular precursors.

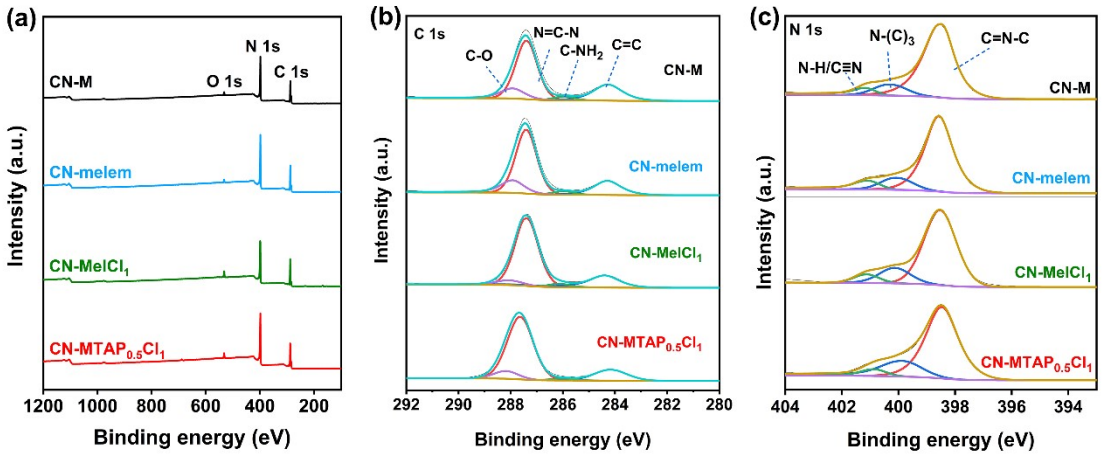

Figure S6 (a) Global XPS spectra, (b) High-resolution C1s XPS spectra and (c) High-resolution N1s XPS spectra of CN-M, CN-melem, CN-$MelCl_1$ and CN-$MTAP_{0.5}Cl_1$.

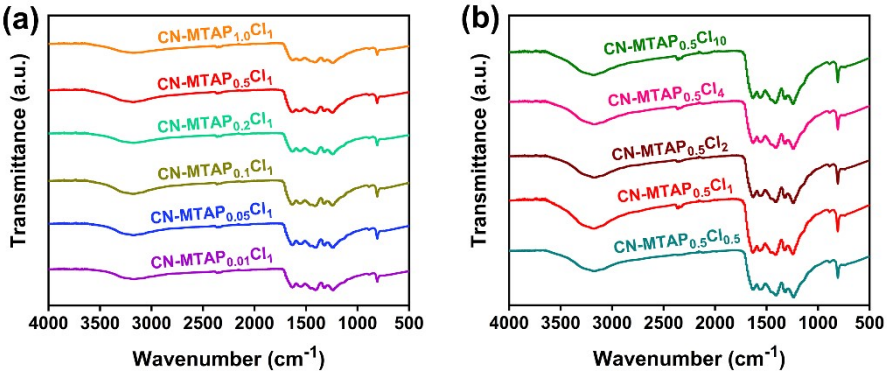

Figure S7. FTIR spectra of CN samples synthesized from (a) $MTAP_xCl_1$ and (b) $MTAP_{0.5}Cl_y$ supramolecular precursors.

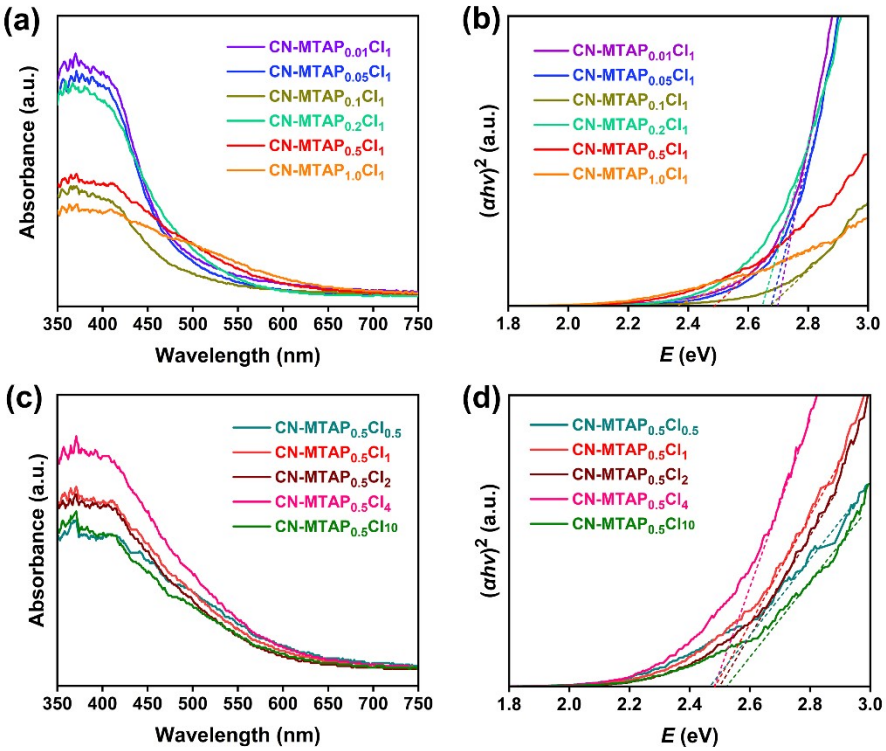

Figure S8. (a, c) UV-vis DRS spectra and (b, d) Corresponding Tauc plots of CN-$MTAP_xCl_1$ and CN-$MTAP_{0.5}Cl_y$.

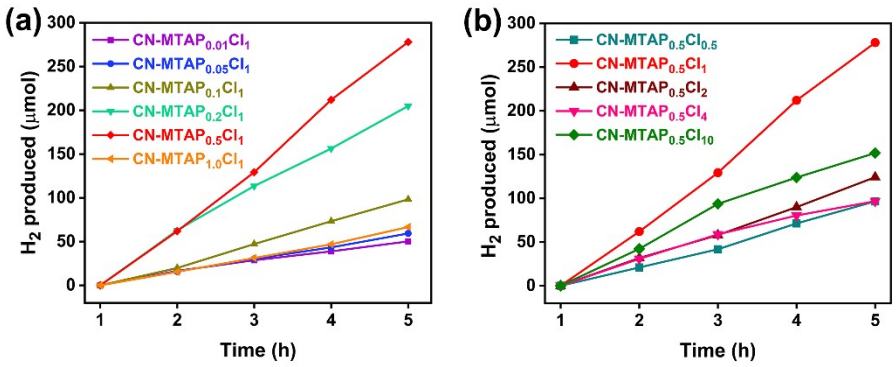

Figure S9 Photocatalytic performance for H2 evolution via water splitting over (a) CN-MTAP$_x$Cl$_1$ and (b) CN-MTAP$_{0.5}$Cl$_y$.

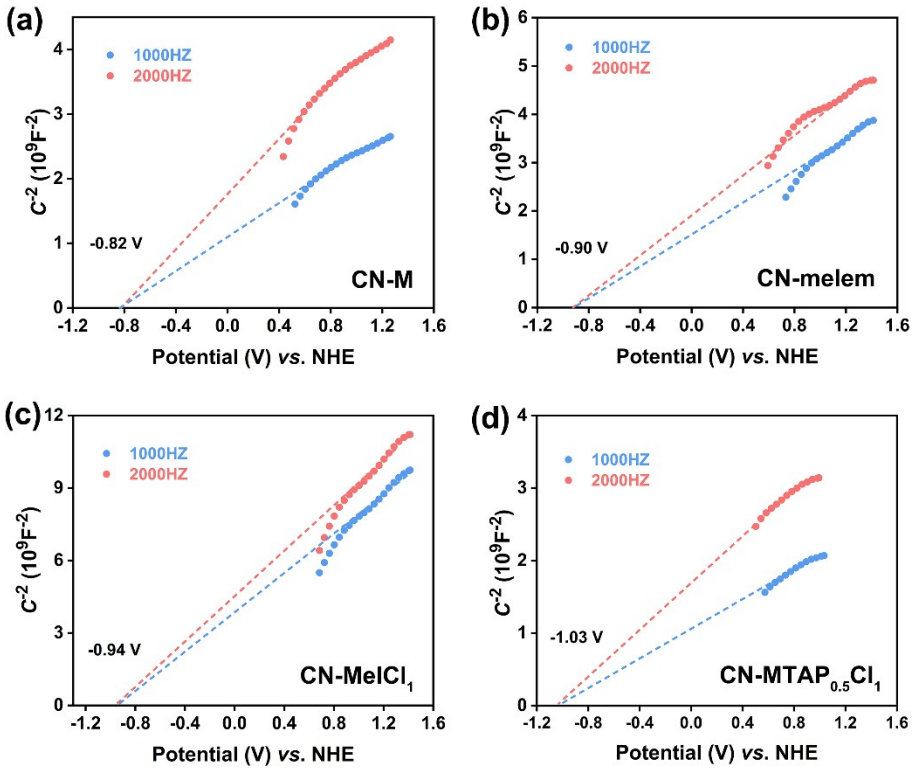

Figure S10. Mott-Schottky measurements of (a) CN-M, (b) CN-melem, (c) CN-MelCl$_1$ and (d) CN-MTAP$_{0.5}$Cl$_1$.

Table S1. Activity comparison of the CN photocatalysts synthesized via supramolecular assembly technique for the hydrogen evolution reaction (HER).

Catalyst	Method	Light source	Catalyst mass	Experimental conditions	Hydrogen evolution rate ($\mu mol\ g^{-1}\ h^{-1}$)	AQE (%)	Ref.
C-doped CN	Thermal condensation of the supramolecular precursor of C-doped melem with HCl (Bridged via H-Cl bond)	300 W Xe lamp ($\lambda \geq 420$ nm), 25 °C	30 mg	3 wt% Pt, 10 vol% TEOA	2316.3	16.0 (λ = 405 nm) 4.7 (λ = 435 nm) 2.0 (λ = 450 nm)	This work
NH2-rich CN	Thermal condensation of supramolecule of melem with HX (Bridged via H-X bond, X = Cl, Br, I)	100 W white LED ($\lambda \geq 400$ nm); 25 °C	15 mg	3 wt% Pt, 10 vol% TEOA	8950	11.5 (λ = 420 nm)	1
Surface nitrogen defect modified crystalline carbon nitride spheres	Quick thermal treatment of CCN synthesized by heating cyanuric acid-melamine supramolecule in molten salt (Bridged via H bond)	300 W Xe lamp ($\lambda > 420$ nm) 15 °C	50 mg	1 wt% Pt, 10 vol% TEOA	1664	1.25 (λ = 420 nm)	2
Boron-doped g-C_3N_4 porous nanotube	Thermal condensation of the supramolecule of melamine, cyanuric acid and boric acid (Bridged via H bond)	36 W LED; 5 °C	50 mg	3 wt% Pt, 20 vol% TEOA	53.2	/	3
Carbon nitride tubular sponges	Thermal condensation of the supramolecule of melamine and phenylphosphonic acid (Salt formation)	300 W Xe lamp ($\lambda > 420$ nm)	20 mg	3 wt% Pt, 15 vol% TEOA	864.9	/	4

Carbon nitride homojunction	Thermal condensation of mixed supramolecules of melamine-cyanuric acid and melamine-thiocyanuric acid (Bridged via H bond)	300 W Xe lamp (λ > 420 nm); 25 °C	33 mg	3 wt% Pt as cocatalyst, 20 vol% TEOA	2875	8.49 (λ = 420 nm)	5
Supramolecular carbon nitride nanoarchitectonics	Thermal condensation of the supramolecule of thiourea and trimesic acid (Bridged via H bond)	450 W Xe lamp 25 °C	100 mg	3 wt% Pt, 10 vol% TEOA	1450	/	6
Hexagonal hollow porous tubular graphitic carbon nitride with rich-π-electrons	Thermal condensation of the supramolecule of melamine and isoniotinic acid (Bridged via H bond)	300 W Xe lamp ($\lambda \geq$ 420 nm) 25 °C	10 mg	0.5 wt% Pt, 10 vol% TEOA	2010	/	7
$AHCN_2$	Thermal condensation of acetamide-urea solid precursor	300 W Xe lamp (λ > 400 nm) 6 °C	10 mg	3 wt.% Pt, 10 vol.% TEOA	5400	15.8 (λ = 400 nm)	8
Ultrathin porous carbon nitride	Condensation of a supramolecules of melamine with β-alanine (lysine, histidine, glutamic acid, methionine, para-aminobenzoic acid) (Bridged via H bond)	300 W Xe lamp (λ > 400 nm) 25 °C	10 mg	3 wt.% Pt, 10 vol.% TEOA	8656	4.03 (λ = 420 nm)	9
Carbon defective g-C_3N_4 thin-wall tubes	Thermal condensation of the supramolecule of melamine with cyanuric acid	300 W Xe lamp (λ > 420 nm)	30 mg	1 wt.% Pt, 10 vol.% TEOA	1647	16.64 (λ = 356 nm) 2.87 (λ = 420 nm)	10
Molybdenum oxide anchored on carbon nitride	Thermal condensation of the supramolecule of cyanuric acid, thiourea and melamine (Bridged via H bond) followed by coupling with molybdenum oxide	300 W Xe lamp (λ > 400 nm), 25 °C	5 mg	1 wt.% Pt, 20 vol.% TEOA	11449	/	11

Dot-like graphitic CN	Thermal condensation of supramolecules of melamine with haloid acids	100 W white LED (λ > 410 nm); water bath, 25 °C	15 mg	3 wt.% Pt, 10 vol.% TEOA	1815	3.2 (λ = 405 nm) 2.1 (λ = 455 nm)	12

Supporting Information References

[1] G. Mark, S. Mondal, M. Volokh, J. Xia, M. Shalom, Halogen-hydrogen bonding for the synthesis of efficient polymeric carbon-nitride photocatalysts, *Solar RRL,* 2022, **6**, 2200834.

[2] L. Fan, Y. Cao, Y. Jia, R. Zhu, D. Zhang, X. Liu, Surface nitrogen defect modified crystalline carbon nitride spheres with boosted carrier dynamics for efficient solar hydrogen production, *Sep. Purif. Technol.,* 2025, **354**, 129254.

[3] S. Zhang, C. An, R. Zhang, D. Kong, D. Xu, S. Zhang, Template-free synthesis of boron-doped graphitic carbon nitride porous nanotubes for enhanced photocatalytic hydrogen evolution, *Langmuir,* 2024, **40**, 6453.

[4] W. Xing, C. Liu, C. Gao, X. Jin, F. Feng, X. Zhang, G. Wu, Polymeric carbon nitride tubular sponges with edge functionalized phosphonic groups for photocatalysis, *J. Inorg. Organomet. P.,* 2024, **34**, 4632.

[5] H. W. Zhang, Y. Y. Li, B. Li, J. H. Shi, T. Huang, G. F. Huang, A. Pan, W. Hu, W. Q. Huang, Competitive assembling strategy to construct carbon nitride homojunctions for boosting photocatalytic performance, *J. Mater. Sci. Technol.,* 2024, **172**, 23.

[6] N. Panangattu Dharmarajan, M. Fawaz, C. I. Sathish, S. N. Talapaneni, K. Ramadass, A. M. Sadanandan, X. M. C. Ta, M. Huš, V. Perumalsamy, A. Tricoli, B. Likozar, C. H. Jeon, J. H. Yang, A. Vinu, Insights into atomic level π-electron modulations in supramolecular carbon nitride nanoarchitectonics for sustainable green hydrogen production, *Adv. Energy Mater.,* 2024, **14**, 2400686.

[7] X. Lin, Y. Ke, Y. Liu, X. Li, Z. Yu, D. Jiang, Y. Yuan, Hexagonal hollow porous tubular graphitic carbon nitride with rich-π-electrons for enhanced photocatalytic hydrogen evolution, *Int. J. Hydrogen Energy,* 2024, **80**, 1234.

[8] X. Zhang, G. Yang, J. Meng, L. Qin, M. Ren, Y. Pan, Y. Yang, Y. Guo, Acetamide- or formamide-assisted in situ approach to carbon-rich or nitrogen-deficient graphitic carbon nitride for notably enhanced visible-light photocatalytic redox performance, *Small,* 2023, e2208012.

[9] W. Zeng, Y. Dong, X. Ye, X. Guan, T. Zhang, L. Guo, Ultrathin porous carbon nitride with molecular structure regulation for excellent photocatalytic water splitting, *Chem. Eng. J.,* 2023, **468**, 143604.

[10] B. Yang, J. Han, Q. Zhang, G. Liao, W. Cheng, G. Ge, J. Liu, X. Yang, R. Wang, X. Jia, Carbon defective g-C_3N_4 thin-wall tubes for drastic improvement of photocatalytic H_2 production, *Carbon,* 2023, **202**, 348.

[11] M. Jourshabani, M. R. Asrami, B. K. Lee, Molecular-level design of isolated molybdenum oxide anchored on carbon nitride for photocatalytic H_2 production and environmental remediation, *Appl. Catal. B,* 2023, **336**, 122907.

[12] J. Barrio, A. Grafmüller, J. Tzadikov, M. Shalom, Halogen-hydrogen bonds: A general synthetic approach for highly photoactive carbon nitride with tunable properties, *Appl. Catal., B* 2018, **237**, 681.